White Dwarfs as Probes of Fundamental Physics: Tracers of Planetary, Stellar and Galactic Evolution
Proceedings IAU Symposium No. 357, 2019
M. A. Barstow, S. J. Kleinman, J. L. Provencal & L. Ferrario, eds.
doi:10.1017/S1743921320000307

Laboratory studies of Vacuum Ultra-Violet (VUV) emission spectra of heavy element ions

W.-Ü Lydia Tchang-Brillet[1], Ali Meftah[1,2], Djamel Deghiche[2], Jean-François Wyart[1,3], Christian Balança[1], Norbert Champion[1] and Christophe Blaess[1]

[1]Laboratoire d'Etude du Rayonnement et de la Matière en Astrophysique et Atmosphèère (LERMA), Observatoire de Paris-Meudon, PSL Research University; Sorbonne Universités, CNRS, F-92190 Meudon, France
email: lydia.tchang-brillet@obspm.fr

[2]Laboratoire de Physique et Chimie Quantique, University Mouloud Mammeri Tizi-Ouzou, Algeria

[3]Laboratoire Aimé Cotton, CNRS UMR9188, Univ Paris-Sud, Univ Paris-Saclay, bâtiment 505, 91405 Orsay CEDEX, France

Abstract. Reliable spectroscopic data are needed for interpretation and modeling of observed astrophysical plasmas. For heavy element ions, which have complex spectra, experimental data are rather incomplete. To provide valuable fundamental quantities, such as precise wavelengths, level energies and semi-empirical transition probabilities, we are carrying out laboratory studies of high-resolution VUV emission spectra of moderately charged ions of transition metals and rare earth elements. Experimental and theoretical methods are summarized. Examples of studies are described.

Keywords. heavy elements, spectra, energy levels, transition probabilities, vacuum ultraviolet

1. Introduction

A huge amount of spectroscopic and collisional data is needed for collisional-radiative modeling of astrophysical plasmas in non-local thermal equilibrium (NLTE) conditions. In particular, heavy elements like transition metals and lanthanides of different ionization stages have attracted attention since their detection in high resolution observational spectra collected in the ultraviolet (UV) region by Hubble Space Telescope (HST/GHRS and STIS). For instance, singly and doubly charged transition metals and lanthanides are present in atmospheres of chemically peculiar stars (See Ryabchikova *et al.* 2006). Spectral lines from Fe V and Ni V observed in white dwarf spectra have been used to test the variation of the fine structure constant α versus gravitation (Prevals *et al.* 2013). Lanthanide and actinide ions up to three times charged are predicted to be formed through the r-process in neutron star mergers, and to strongly contribute to the opacity of the ejected matter (Karsen*et al.* 2013).

The present contribution aims to summarize experimental and parametric studies of triply and quadruply charged lanthanide ions, carried on within our collaborating team. After Nd IV (Wyart *et al.* 2007) and Nd V (Meftah *et al.* 2008; Deghiche *et al.* 2015), followed by Tm IV (Mefta *et al.* 2007), Yb V (Meftah *et al.* 2013) and Er IV (Meftah *et al.* 2016), extensions to other Thulium ions and to higher configurations of Nd IV (Arab *et al.* 2019) are underway. The electronic configurations of these ions have $5p^6 4f^N$

and $4f^{N-1}nl$, $5p^5 4f^N nl$ open subshells, which result in dense and complex spectra in the vacuum ultraviolet (VUV) wavelength range (300–3000Å). To disentangle these spectra in the laboratory and to derive energy levels and fundamental properties of these ions, high spectral resolution is needed and a systematic isoelectronic or isoionic approach is helpful.

Although *ab initio* theoretical calculations provide a great amount of atomic data needed, experimental studies remain essential. For instance, in Nd IV, a recent full relativistic *ab initio* calculation (Gaigalas *et al.* 2019) led to calculated wavelengths with deviations within 20% from the experimental ones (Wyart *et al.* 2007). Indeed, a precision of 10^{-6} on VUV wavelengths can only be achieved by experimental measurements. The knowledge of experimental energy levels is a starting point for validation of *ab initio* calculations. Furthermore, reliable semi-empirical radiative transition probabilities and Landé factors can be derived from parametric calculations based on experimental energies (see below). In Nd IV, a comparison of gA values (weighted probability for spontaneous emission) from Cowan's code parametric calculations (Arab *et al.* 2019) and from a more sophisticated semi-empirical calculation (Enzonga Yoca & Quinet 2014) fitting the same experimental energies agree within 10%, whereas the full relativistic *ab initio* values of gA may deviate by a factor 2 (Gaigalas *et al.* 2019).

2. Experimental methods

We record emission spectra on the 10.7-meter high-resolution normal incidence VUV spectrograph of the Meudon Observatory. This instrument is equipped with a 3600 lines/mm holographic concave grating, leading to a linear dispersion of 0.25 Å/mm in the focal plane in the first order. The resulting resolution is about 150 000 with a slit width of 30 μm. The plate-holder was designed to accommodate two photographic plates of 18″ x 2″, allowing simultaneous recording of a wavelength range of 240 Å between 300 and 3000 Å. Photographic plates provide precise wavelength measurements but they are no longer available. Instead, we use photo-stimulable image plates, which show enough sensitivity in the VUV range (Reader *et al.* 2000). They have linear response in intensity over five orders of magnitude. Indeed, a succession of CCDs paving the focal plane would have been too expensive and yet unsatisfactory with respect to resolution and focusing onto the Rowland circle. Emission spectra of ionized lanthanides are produced using high-voltage low inductance vacuum spark sources with an anode made of the element of interest. By varying the peak electric current, it is possible to discriminate lines from different ionization stages, generally three of them, according to their intensity behaviors. Impurity lines with well known wavelengths are used as internal standards for wavelength calibration of the spectrograms. The uncertainties of the measured wavelengths are estimated to be $\pm 0.001 - 0.005$Å. Figure 1 displays two wavelength sections of experimental thulium spectra recorded on image plates.

3. Analysis and parametric calculations

The analysis of a complex spectrum aims for determination of the energy level scheme of the ion from the observed lines by applying the Ritz combination principle taking into account selection rules on quantum numbers for electric dipole transitions. For each transition between one upper level and one lower level of opposite parities, $\Delta E = E_u - E_l = \sigma$, where σ is the wavenumber of the line and E, the energy value of a level in cm^{-1}. Furthermore, the observed intensities must be consistent with theoretical predictions of transition probabilities. Consequently, the analysis must be supported by theoretical studies. We apply the Racah-Slater semi-empirical method, by means of Cowan's codes (RCN/RCN2/RCG/RCE) (Cowan 1981).

https://doi.org/10.1017/S1743921320000307 Published online by Cambridge University Press

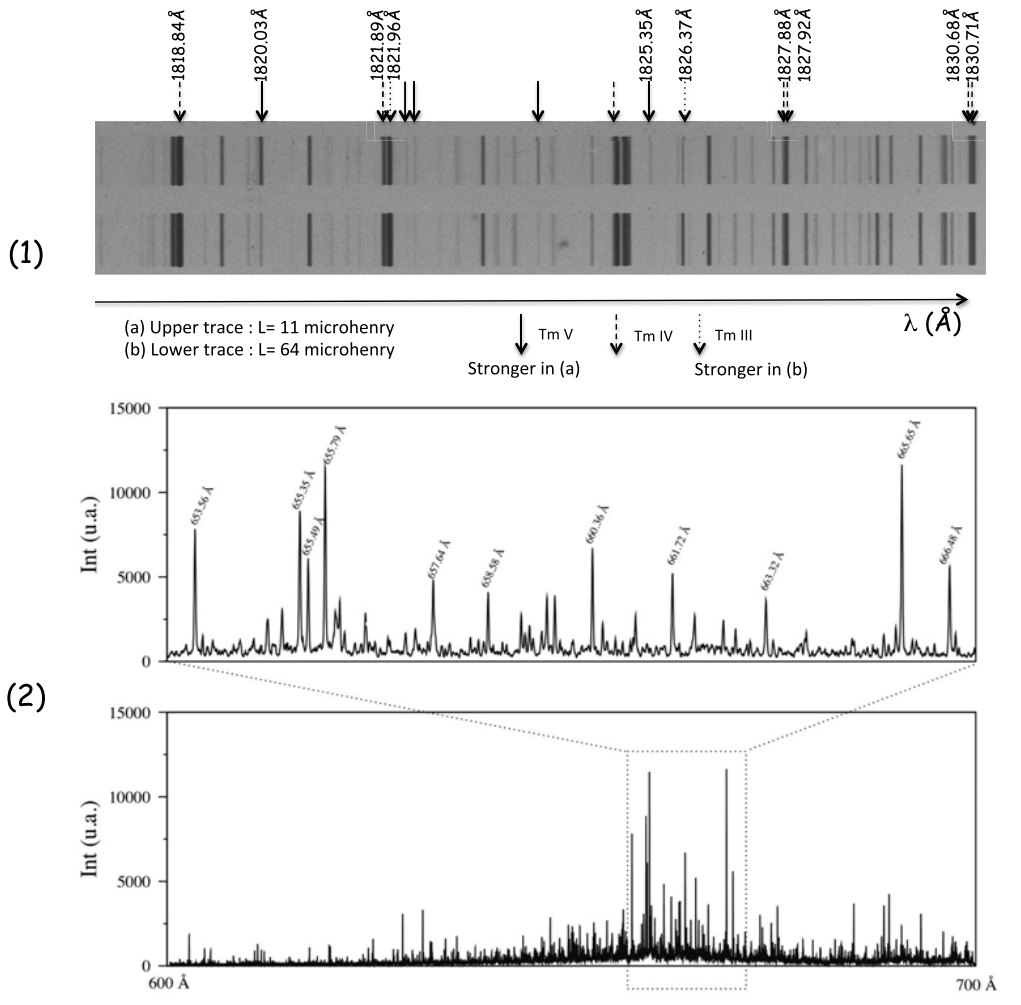

Figure 1. Sections of the thulium vacuum spark emission spectrum. (1) Spectra recorded on image plates in two different discharge conditions, showing different behaviors of Tm III – V lines (1815 – 1830 Å); (2) Digitized intensity profiles in a shorter wavelength region (600 – 700 Å) showing mainly Tm V lines in the enlarged section.

In the first step, *ab initio* predictions of level energies from unknown configurations and transition probabilities are derived by Hartree-Fock calculations including relativistic corrections (HFR). The Hamiltonian is diagonalized in the basis of one or several configurations, to explicitly take into account configuration interactions. Matrix elements are written as a sum of products of an angular part c_{ij}^{α} given by Racah algebra and a radial integral P_{α}: $H_{ij} = \sum_i c_{ij}^{\alpha} P_{\alpha}$.

A second semi-empirical step is performed as soon as some experimental values of energies become available. The radial integrals P_{α} are treated as adjustable energy parameters in a least square fit (LSQ) minimizing the mean standard deviation ΔE defined as : $\Delta E = \sqrt{(N_l - N_P)^{-1} \sum_s i(E_i^{exp} - E_i^{calc})^2}$ where N_l is the number of fitted levels and N_P the number of parameters. An iteration of the cycle LSQ/diagonalization provides improved predictions for unknown levels and line intensities. One may mention a few refinements in the present approach. Most of the time, the HFR values of average

https://doi.org/10.1017/S1743921320000307 Published online by Cambridge University Press

Table 1. Identified transitions in Tm V used for the determination of three $4f^{10}6p$ levels.

$E_u(cm^{-1})$	J_u	$4f^{10}6p$ term	$\lambda(\mathring{A})$	$\sigma(cm^{-1})$	Int^1_{exp}	$gA(s^{-1})$	$E_l(cm^{-1})$	J_l	$4f^{10}(5d+6s)$ term
249871.29	7.5	^6H	896.49	111546.14	150	1.585E+10	138325.83	7.5	^6H
			900.59	111038.31	157 p	8.208E+09	138833.94	8.5	^6I
			906.20	110350.91	141	1.989E+10	139521.49	6.5	^6G
			1837.74	54414.58	181	9.472E+09	195456.43	8.5	^6I
			1903.77	52527.23	22	2.197E+09	197343.07	7.5	^4I
250401.53	8.5	^4K	892.25	112076.21	45	7.533E+09	138325.83	7.5	^6H
			896.32	111567.29	169	1.536E+10	138833.94	8.5	^6I
			918.04	108927.71	180	2.331E+10	141474.16	9.5	^6K
			959.40	104231.81	38	2.887E+09	146171.21	9.5	^6K
			1820.03	54943.94	156	6.833E+09	195456.43	8.5	^6I
			1884.74	53057.54	121	5.137E+09	197343.07	7.5	^4I
257574.44	7.51	^6K	893.63	111903.42	51	3.305E+09	145671.02	8.5	^4K
			893.52	111916.91	103	1.031E+10	145657.94	7.5	^6H
			922.68	108379.89	223	1.989E+10	149195.71	8.5	^6L
			931.53	107349.37	47	3.860E+09	150226.91	7.5	^4I

Notes: [1]Experimental intensities in arbitrary units, estimated from the area under the line profile.
p: perturbed

energies of configurations, E_{av}, need to be scaled according to the observed positions of transition arrays on the wavenumber scale, which indicate the relative distances between configurations. Furthermore, the HFR values of radial integrals (electrostatic and spin-orbit) are overestimated and need to be scaled by an appropriate scaling factor (SF) derived from neighboring ions. Indeed, isoelectronic or isoionic ions show rather consistent values of scaling factors and provide reliable choices for initial parameter values of the LSQ fit (Wyart 2011). This allows reliable correspondences between experimental and calculated energies in the fit, in case of very close levels of the same J.

Analyses have gained efficiency using the interactive IDEN code (Azarov 1993; Azarov *et al.* 2018) based on pattern recognition with visual display of the experimental data together with the predictions of the Cowan codes on level energies, wavenumbers, and line intensities. The final experimental energy values are optimized by using the LOPT code (Kramida 2011), which minimizes the differences between the whole set of wavenumbers from wavelength measurements and those calculated from the experimental energies by the Ritz principle (Ritz wavelengths). These latter generally have reduced uncertainties compared to the observed wavelengths.

4. Example results

As an example of typical results derived from spectral analyses, Table 1 shows preliminary results on the Tm V spectrum analysis. For three previously unknown levels of $4f^{10}6p$, the experimental energy, the quantum number J, the wavelengths and wavenumbers of transitions involved in their determinations are reported, together with their intensities compared to calculated transition probabilities gA, the energy and designation of the lower level. Complete results on energy levels, line list and parameter values will be published later elsewhere.

Our previously published data are available on the https://molat.obspm.fr webpage.

References

Arab, K., Deghiche, D., Meftah, A., Wyart, J.-F., Tchang-Brillet, W.-Ü. L., Champion, N., Blaess, C., & Lamrous, O. 2019, *JQSRT*, 229, 145

Azarov, V. I. 1993, *Physica Scripta*, 48, 656

Azarov, V. I., Kramida, A., & Vokhmentsev, M. Ya 2018, *Comput. Phys. Comm.*, 225, 149

https://doi.org/10.1017/S1743921320000307 Published online by Cambridge University Press

Cowan, R. D. 1981 *The Theory of Atomic Structure and Spectra*, University of California Press
Deghiche, D., Meftah, A. Wyart, J.-F., Champion, N., Blaess, C., & Tchang-Brillet, W.-Ü. L. 2015, *Physica Scripta*, 90, 095402
Enzonga Yoca, S. & Quinet, P. 2014, *J. Phys. B Atomic Molecular Physics*, 47, 035002
Gaigalas, G., Kato, D., Rynkun, P., Radziute, L., & Tanaka, M. 2019, *ApJS*, 240, 29
Kasen, D., Badnell, N. R., & Barnes, J. 2013, *ApJ*, 774, 25
Kramida, A. E. 2011, *Computer Physics Communications*, 182, 419
Meftah, A., Wyart, J.-F., Champion, N., & Tchang-Brillet, W.-Ü. L. 2007, *European Physical Journal D*, 44, 35
Meftah, A., Wyart, J.-F., Sinzelle, J., Tchang-Brillet, W.-Ü. L., Champion, N., Spector, N., & Sugar, J. 2008, *Physica Scripta*, 77, 055302
Meftah, A., Wyart, J.-F., Tchang-Brillet, W.-Ü. L., Blaess, C., & Champion, N. 2013, *Physica Scripta*, 88, 045305
Meftah, A. *et al.* 2016, *J. Phys. B*, 49, 5002
Preval, S. P., Barstow, M. A., Holberg, J. B., & Dickinson, N. J. 2013, *MNRAS*, 436, 659
Reader, J., Sansonetti, C. J., & Deslattes, R. D. 2000, *Applied Optics*, 39, 637
Ryabchikova, T., Ryabtsev, A., Kochukhov, O., & Bagnulo, S. 2006, *A&A*, 456, 329
Wyart, J.-F., Meftah, A., Tchang-Brillet, W.-Ü. L., Champion, N., Lamrous, O., Spector, N., & Sugar, J. 2007, *J. Phys. B Atomic Molecular Physics*, 40, 3957
Wyart, J.-F. 2011, *Canadian Journal of Physics*, 89, 451